



Integral Transforms with Single Domain Formulation for Transient Three-Dimensional Conjugated Heat Transfer

Adam H. R. Sousa, Kleber M. Lisboa, Carolina P. Naveira-Cotta & Renato M. Cotta

To cite this article: Adam H. R. Sousa, Kleber M. Lisboa, Carolina P. Naveira-Cotta & Renato M. Cotta (2023): Integral Transforms with Single Domain Formulation for Transient Three-Dimensional Conjugated Heat Transfer, Heat Transfer Engineering, DOI: [10.1080/01457632.2023.2178277](https://doi.org/10.1080/01457632.2023.2178277)

To link to this article: <https://doi.org/10.1080/01457632.2023.2178277>



Published online: 02 Mar 2023.



Submit your article to this journal [↗](#)



Article views: 42






View related articles [↗](#)



View Crossmark data [↗](#)



Integral Transforms with Single Domain Formulation for Transient Three-Dimensional Conjugated Heat Transfer

Adam H. R. Sousa^a, Kleber M. Lisboa^b , Carolina P. Naveira-Cotta^a , and Renato M. Cotta^{a,c} 

^aLabMEMS - Laboratory of Nano & Microfluidics and Microsystems, Mechanical Engineering Department, DEM/PEM, POLI/COPPE, Federal University of Rio de Janeiro, UFRJ, Rio de Janeiro, RJ, Brazil; ^bLATERMO - Laboratory of Thermal Sciences, Mechanical Engineering Department, TEM/PGMEC, Universidade Federal Fluminense, UFF, Niterói, RJ, Brazil; ^cLATES - Laboratory of Technologies for Sustainable Energies, LATES, Materials Group, Navy Research Institute, IPqM, General Directorate of Nuclear and Technological Development, DGDNTM, Brazilian Navy, Ministry of Defense, Rio de Janeiro, RJ, Brazil

ABSTRACT

An analysis based on integral transforms is undertaken for transient three-dimensional conjugated conduction-convection heat transfer, with a focus on mini or micro channels-based devices. The numerical-analytical approach Generalized Integral Transform Technique (GITT) is combined with a single domain reformulation, providing accurate, robust, and cost-effective simulations for determining temperature distributions within the domain. The fluid and solid subdomains are represented as one single region, while the integral transformation is carried out using a three-dimensional eigenvalue problem encompassing the thermophysical properties and velocity field abrupt spatial variations. The steady state problem solution is employed as a filter and solved through an integral transformation based on the corresponding two-dimensional eigenvalue problem defined for the channel cross section. The transformed ordinary differential systems for both the steady and homogeneous transient problems are handled analytically, requiring only the numerical solution of the associated matrix eigensystem analysis. Converged numerical results for dimensionless temperature distributions are then critically compared with a finite element solution and a previously proposed GITT solution that implements a partial transformation scheme under a pseudo-transient formulation, both for the conjugated problem with thermally developing laminar flow in a rectangular channel.

Introduction

Conjugated conduction-convection heat transfer is one of the most classical problem formulations in thermal sciences. While an exact solution is not yet available to the general situation, a few approximate analytical solutions have been proposed throughout the last few decades, since the pioneering works of Perelman [1] and Luikov et al. [2], especially for two-dimensional steady formulations, either as fully differential or mixed lumped-differential models. Applications are numerous, in both the physical sciences and engineering contexts, appearing whenever solid structures or flow inserts cannot be disregarded when analyzing the heat transfer process in the whole fluid-solid thermal system. Then, classical correlations or analytical solutions for purely convective heat transfer are no longer applicable, and computational fluid mechanics tools are forcedly required to provide

costly numerical solutions to such inherently conjugated problems.

Microfluidics is a fairly recent scientific domain characterized by fluid flow and heat and mass transfer at the micro-scale and the associated applications [3–5]. A literature survey on Google Scholar with the keyword “microfluidics”, which includes journal papers, conferences and patents, results in an ever-increasing number of documents since 1981, with a marked increase after the years 2000, and more than 20,000 documents per year in 2020 [6]. Process intensification is the main drive behind this miniaturization wave of various classes of devices, including micro-mixers, micro-pumps, micro-separators, micro-reactors, microfluidic batteries, and micro-heat exchangers, among others. An increasing focus in the research on heat and mass transfer at the micro-scale, with focus on such different micro-devices, has been evident in the open literature in

Nomenclature

A	Area of the cross section of the channel, m^2	β, ν, μ, λ	Eigenvalues associated to eigenfunctions ξ, Ω, Ψ, χ , respectively
AR	Aspect ratio	Γ, ω	Auxiliary eigenfunctions
c	Coefficients of the solution of the first order transformed problem	$\delta_{i,j}$	Kronecker's delta
c_p	Specific heat, J/kgK	ζ	Matrix of eigenvectors of L
D_h	Hydraulic diameter, m	ξ	Eigenvectors of L
GITT	Generalized Integral Transform Technique	θ	Dimensionless temperature profile
ITRS	International Technology Roadmap for Semiconductors	ξ, Ω	Eigenfunctions of the steady conjugated problem
k	Thermal conductivity, W/mK	ρ	Density, kg/m^3
K	Dimensionless thermal conductivity	σ_x	Ratio between the hydraulic diameter and the width of the device
L	Coefficients matrix for the first order transformed problem	σ_y	Ratio between the hydraulic diameter and the height of the device
L_{xT}	Microfluidic apparatus width in x direction, m	τ	Dimensionless time
L_{yT}	Microfluidic apparatus width in y direction, m	Φ	Vector of dependent functions
L_{xM}	Microchannel width in x direction, m	ψ, χ	Eigenfunctions of the homogeneous transient conjugated problem
L_{yM}	Microchannel width in y direction, m		
N	Normalization integrals		
ODE	Ordinary Differential Equation		
PDMS	Polydimethylsiloxane	Subscripts	
Pe	Péclet number	av	Related to the average field
t	Time variable, s	f	Fluid region
T	Temperature, $^{\circ}C$	H	Related to the homogeneous transient problem
\mathbf{u}	Velocity vector, m/s	i, k, m, n	Indices associated with the eigenvalue problems
u	Velocity component along the z-direction, m/s	in	Related to the inlet conditions
U	Dimensionless velocity component along the z-direction	P	Related to the steady state problem
w	Volumetric heat capacity (ρc_p), J/m^3K	s	Solid region
W	Dimensionless volumetric heat capacity	w	Related to the channel wall
x, y, z	Coordinates, m	x	Refers to the x-direction
X, Y, Z	Dimensionless coordinates	y	Refers to the y-direction
z_{∞}	Length of the device, m		
Z_{∞}	Dimensionless length of the device	Superscripts	
		\sim	Normalized eigenfunction
		$-$	Transformed potential
Greek symbols			
α	Thermal diffusivity, m^2/s		
α_j	Eigenvalues of matrix L		

recent decades, driven by the ever-growing demand for lighter, smaller and more efficient micro-systems [5, 7–10]. For instance, since the pioneering work of Tuckerman and Pease [11], the reduced size of the channels and the associated rise in heat dissipation capacity, rendered micro-heat exchangers an interesting option for the cooling of electronic devices. In 2012, the *International Technology Roadmap for Semiconductors* (ITRS) anticipated that, in 2020, the dissipated power of integrated circuits would be above $100 W/cm^2$ [12]. Since then, three-dimensional integrated circuits have been advanced, outpacing ITRS roadmap forecasts, while requiring cooling based on an interlayer microchannels structure [13–15]. In addition, single phase microchannels-based heat exchangers have been the preferred option in several heat removal intensive applications, ranging from high concentration photovoltaics, 3D chip stacks, fuel cells, micro-reactors, among others [12, 16–23].

Along the development of micro-devices that involve heat transfer, deviations have been observed between experimental and theoretical results of important performance parameters [24, 25], which have been diminishing in recent years, largely on account of advances in measurement techniques. Nonetheless, discrepancies were also observed while adopting correlations originally derived from macro-scale experiments to verify quantities in microchannels measurements, pointing out to the necessity of proposing specific correlations for microscale devices. One of the claims is that such deviations can be mainly attributed to disregarding phenomena that, differently from the macroscale, may have significant importance in a thermal microsystem. These effects are known as scaling effects, such as wall conjugation, viscous dissipation, entry effects, measurement uncertainty, axial heat diffusion, slip and temperature jump, compressibility, among others [10, 24, 26–33]. There

is still a disagreement in the literature regarding which scaling effects are essential on the correct treatment of heat transfer problems at the microscale, for each specific application, but there is strong evidence that the conjugation effect is highly relevant and its influence must be, at least, checked for in every case [10, 27, 28, 31]. Thus, a better agreement between experimental and simulation results for convective heat transfer in microchannels requires research on models and solution methodologies that are capable of adequately describing the relevant physical phenomena to fluid flow and heat transfer at such scales.

Not rarely, the solid substrates and the channels of thermal micro devices are of comparable sizes, and, besides, due to combinations of physical dimensions and properties, in general participate in the overall heat transfer process. Thus, for the theoretical analysis, design and optimization of micro-devices that involve heat transfer, it is commonly mandatory to study the conjugated heat transfer problem. As previously mentioned, since the general class of conjugated conduction-convection problems in full partial differential formulation does not have known exact analytical solutions, purely numerical or hybrid (numerical-analytical) methods are possible alternatives. However, due to the presence of multiple geometric scales and abrupt interfaces between distinct materials, purely numerical approaches in general require refined discretization meshes in different sub-regions and their transitions, which results in considerable computational costs. In addition, purely numerical schemes suffer from soaring computational costs when dealing with three-dimensional formulations. Therefore, previous works have dealt with hybrid numerical-analytical solutions for this class of conjugated problems, offering robustness, accuracy and, in particular, mild computational effort. This aspect becomes more evident in highly intensive computational tasks, such as in optimization, inverse problems, and simulation under uncertainty, when a very large number of runs in the direct problem solution is required. One such hybrid approach is known as the Generalized Integral Transform Technique - GITT [34–43] which derives from the Classical Integral Transform Method, Mikhailov and Ozisik [44]. The GITT offers solutions with robustness and error control similar to its purely analytical version, significantly expanding the coverage of this more flexible hybrid method in different classes of problems that are, in principle, non-transformable in the analytical sense. The GITT solution of conjugated problems was first proposed in the realm of periodic convection

with conjugation effects in the form of just a transversal thermal resistance but considering the wall thermal capacitance [45, 46]. Soon afterwards, the axial conduction along the wall was considered, but still simplifying the formulation with respect to the transversal wall conduction through a partial lumped analysis [47–49]. This same concept was later extended through an improved lumped-differential analysis [39, 50], being applied and experimentally validated in the analysis of rectangular micro-heat exchangers [51]. The proposition of a single domain reformulation strategy allowed for the solution of full conjugated heat transfer problems through the introduction of spatially variable coefficients without any approximation to the wall heat conduction process [52]. The approach was then extended to include other scaling effects and generalizing the formulation for regular and complex geometries in steady or transient regimes [53–60]. More recently, Knupp et al. [61] developed a convective eigenvalue problem and achieved a convergence acceleration in solving conjugated problems for parallel plate channels via GITT.

Besides extending the integral transform approach to progressively more involved conjugated problem formulations, a few works have previously addressed transient conjugated problems, including periodic disturbances or fluctuations in the flow field, and/or wall and entry conditions, which only under very special circumstances can be reduced to quasi-steady formulations [62–66]. Though a two-dimensional transient formulation [56] and a three-dimensional steady formulation [55] have been previously dealt with GITT, a total transformation scheme for transient three-dimensional conjugated problems has not yet been implemented. As for the full transient formulation in micro heat exchangers, although the reduced spatial scales lead *a priori* to very small-time scales in the convective heat transfer transients, it should be recalled that the substrate thermal capacitance may play a major role in the time evolution of flow or temperature disturbances, requiring the full transient analysis of the thermal problem.

In this context, the present work aims to contribute with a hybrid numerical-analytical solution of a full transient three-dimensional conjugated problem formulation in thermal microsystems, through the combined use of GITT and the single domain reformulation strategy. In microchannels, Reynolds numbers are typically low and characteristic of laminar flows. Also, the hydrodynamic development lengths are in general very small relative to the total length of the exchanger, and the flow entrance effects

are negligible, leading to a thermally developing flow situation. On the other hand, Peclet number may be sufficiently low to require the inclusion of the fluid axial diffusion term in the energy equation. The focus of the present work is the generalization of the hybrid methodology for the treatment, via total transformation, of the transient three-dimensional energy equation, written for both the solid and fluid domains. Following the single domain strategy, the problem is reformulated through unified spatially variable coefficients that include the abrupt spatial variations associated with the properties and velocities of fluid and solid. Thus, the integral transform method solves one single energy equation for the entire region, obtaining the transient temperature field through the expansion of the appropriate three-dimensional eigenfunctions. The spatial variation of the coefficients from the original problem is fully represented within the eigenvalue problem, which is itself solved via GITT due to its inherent complexity and to the inexistence of an analytical solution.

Problem formulation

Consider incompressible laminar flow of a Newtonian fluid inside a rectangular microchannel, with dimensions and coordinates system defined as in Figure 1, and external walls subjected to a prescribed uniform temperature T_w , different from the system initial temperature, T_{in} . Two scaling effects are here considered, namely the wall conjugation and the axial heat diffusion effects. The channel walls participate in the heat transfer process both in the transversal and longitudinal directions. The flow is considered hydrodynamically developed and thermally developing from a uniform inlet temperature, T_{in} , the same as the initial temperature of the whole device, with temperature independent physical properties. The hydrodynamically developed flow assumption is associated with the

presence of an upstream adiabatic channel section where the fully developed flow profile is achieved. Then, the transient three-dimensional conjugated problem is reformulated as a single domain energy equation as:

$$w(x, y) \left[\frac{\partial T}{\partial t} + \mathbf{u} \cdot \nabla T \right] = \nabla \cdot [k(x, y) \nabla T], 0 < x < L_{x_T}, \\ 0 < y < L_{y_T}, 0 < z < z_{\infty}, t > 0 \quad (1a)$$

$$T(0, y, z, t) = T_w; T(L_{x_T}, y, z, t) = T_w; \\ 0 \leq y \leq L_{y_T}, 0 \leq z \leq z_{\infty}, t > 0 \quad (1b,c)$$

$$T(x, 0, z, t) = T_w; T(x, L_{y_T}, z, t) = T_w; \\ 0 \leq x \leq L_{x_T}, 0 \leq z \leq z_{\infty}, t > 0 \quad (1d,e)$$

$$T(x, y, 0, t) = T_{in}; \left. \frac{\partial T}{\partial z} \right|_{z=z_{\infty}} = 0; \\ 0 \leq x \leq L_{x_T}, 0 \leq y \leq L_{y_T} \quad (1f,g)$$

$$T(x, y, z, 0) = T_{in}; 0 \leq x \leq L_{x_T}, 0 \leq y \leq L_{y_T}, 0 \leq z \leq z_{\infty} \quad (1h)$$

The thermophysical properties and the fully developed velocity profile are incorporated into spatially variable coefficients, so as to represent the abrupt transitions between the fluid and solid regions as:

$$k(x, y) = \begin{cases} k_f, & \text{at fluid region} \\ k_s, & \text{at substrate region} \end{cases} \quad (2a)$$

$$w(x, y) = \begin{cases} w_f, & \text{at fluid region} \\ w_s, & \text{at substrate region} \end{cases} \quad (2b)$$

$$u(x, y) = \begin{cases} u_f(x, y), & \text{at fluid region} \\ 0, & \text{at substrate region} \end{cases} \quad (2c)$$

where w_f and w_s are, respectively, the fluid and solid volumetric heat capacities, whereas k_f and k_s are, respectively, the fluid and solid thermal conductivities, and $u_f(x, y)$ is the fully developed velocity

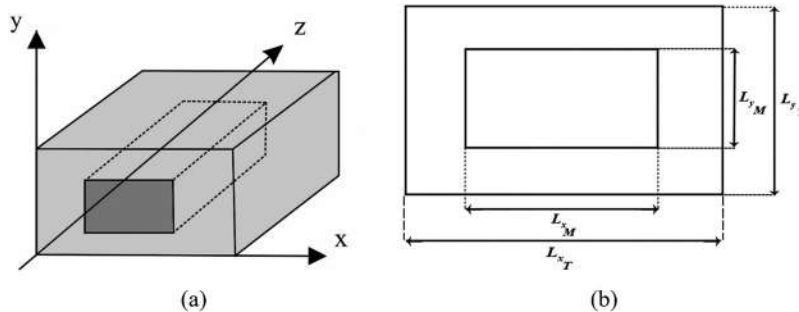


Figure 1. Schematic representation of the transient three-dimensional conjugated problem in a rectangular microchannel and corresponding solid substrate. (a) Coordinates system and (b) Definitions for the height and width of the substrate and microchannel.

profile in the fluid. The dimensionless groups are defined as:

$$W = \frac{w}{w_f}; \theta = \frac{T - T_w}{T_{in} - T_w}; \tau = \frac{\alpha_f t}{D_h^2} \quad (3a-c)$$

$$X = \frac{2x}{L_{xT}}; Y = \frac{2y}{L_{yT}}; Z = \frac{z}{D_h Pe} \quad (3d-f)$$

$$U = \frac{u}{u_{av}}; K = \frac{k}{k_f}; Pe = \frac{u_{av} D_h}{\alpha_f}; \alpha_f = \frac{k_f}{w_f}; D_h = 2 \frac{L_{xM} L_{yM}}{L_{xM} + L_{yM}} \quad (3g-k)$$

$$\sigma_x = \frac{L_{xT}}{D_h}; \sigma_y = \frac{L_{yT}}{D_h}; X_i = \frac{L_{xM}}{L_{xT}}; Y_i = \frac{L_{yM}}{L_{yT}}; AR = \frac{Y_i}{X_i} \quad (3l-p)$$

where u_{av} is the average flow velocity. The dimensionless transversal space variables were taken from 0 to 2 to match the definitions in Ref. [55] for comparison purposes, which employed the limits from 0 to 1, but imposed symmetry of the boundary conditions on the transversal directions. Here, symmetry conditions were not imposed, so as to generalize the approach for non-symmetric boundary conditions and/or channel geometries. Equations (1a-h) can then be rewritten in dimensionless form as:

$$W(X, Y) \left[\frac{\partial \theta}{\partial \tau} + U(X, Y) \frac{\partial \theta}{\partial Z} \right] = \frac{4}{\sigma_x^2} \frac{\partial}{\partial X} \left[K(X, Y) \frac{\partial \theta}{\partial X} \right] + \frac{4}{\sigma_y^2} \frac{\partial}{\partial Y} \left[K(X, Y) \frac{\partial \theta}{\partial Y} \right] + \frac{1}{Pe^2} \frac{\partial}{\partial Z} \left[K(X, Y) \frac{\partial \theta}{\partial Z} \right], \quad 0 < X < 2, \quad 0 < Y < 2, \quad 0 < Z < Z_\infty, \quad \tau > 0 \quad (4a)$$

$$\theta(0, Y, Z, \tau) = 0; \theta(2, Y, Z, \tau) = 0; 0 \leq Y \leq 2, 0 \leq Z \leq Z_\infty, \tau > 0 \quad (4b,c)$$

$$\theta(X, 0, Z, \tau) = 0; \theta(X, 2, Z, \tau) = 0; 0 \leq X \leq 2, 0 \leq Z \leq Z_\infty, \tau > 0 \quad (4d,e)$$

$$\theta(X, Y, 0, \tau) = 1; \frac{\partial \theta}{\partial Z} \Big|_{Z=Z_\infty} = 0; 0 \leq X \leq 2, 0 \leq Y \leq 2, \tau > 0 \quad (4f,g)$$

$$\theta(X, Y, Z, 0) = 1; 0 \leq X \leq 2, 0 \leq Y \leq 2, 0 \leq Z \leq Z_\infty \quad (4h)$$

The dimensionless thermophysical properties and velocity profile are defined, for a straight rectangular channel, as:

$$K(X, Y) = \begin{cases} 1, & 1 - X_i \leq X \leq 1 + X_i, 1 - Y_i \leq Y \leq 1 + Y_i \\ k_f/k_s, & \text{otherwise} \end{cases} \quad (5a)$$

$$W(X, Y) = \begin{cases} 1, & 1 - X_i \leq X \leq 1 + X_i, 1 - Y_i \leq Y \leq 1 + Y_i \\ w_f/w_s, & \text{otherwise} \end{cases} \quad (5b)$$

$$U(X, Y) = \begin{cases} \frac{u_f(x, y)}{u_{av}}, & 1 - X_i \leq X \leq 1 + X_i, 1 - Y_i \leq Y \leq 1 + Y_i \\ 0, & \text{otherwise} \end{cases} \quad (5c)$$

The dimensionless velocity profile is obtained for fully developed flow in a rectangular channel, which has analytical solution by separation of variables, as presented in Ref. [36]:

$$\frac{u_f(x, y)}{u_{av}} = U_f(X, Y) = A^* \sum_{j=1, 3, 5, \dots}^{\infty} B_j F_j(Y) G_j(X) \quad (6a)$$

$$A^* = \frac{48}{\pi^3} \left[1 - \frac{192 X_i}{\pi^5 Y_i} \sum_{l=1, 3, 5, \dots}^{\infty} \frac{1}{l^5} \tanh \left(\frac{l \pi Y_i}{2 X_i} \right) \right]^{-1}; \quad B_j = \frac{(-1)^{(j-1)/2}}{j^3} \quad (6b,c)$$

$$F_j(Y) = 1 - \frac{\cosh(a_j Y)}{\cosh(a_j Y_i)}; G_j(X) = \cos(a_j X); a_j = \frac{j \pi}{2 X_i} \quad (6d-f)$$

Solution methodology

Integral transform solutions for transient conjugated heat transfer in two-dimensional parallel plate channels [56] and for steady-state three-dimensional rectangular channels [54] have been previously obtained. In both works, the partial transformation scheme of the GITT was employed, constructing eigenfunction expansions in the transversal coordinates only, and leaving the axial variable untransformed. Then, a transformed partial differential system results, having the longitudinal coordinate and time (for the transient problem or a pseudo-transient formulation for the steady problem) as independent variables, which is numerically handled to yield the transformed temperatures. The partial transformation path reduces the analytical involvement and, in many cases, competes on computational cost with the more traditional total transformation scheme. Nevertheless, accuracy requirements might favor the adoption of the total transformation alternative, eliminating all the space variables in analytic form and solving an ordinary differential transformed system instead. In addition, for a linear transformed ordinary differential equation

(ODE) system that is analytically solvable, there might be a significant gain in overall computational cost as well. Thus, a total integral transformation scheme combined with the single domain reformulation strategy is here employed in solving transient three-dimensional conjugated problems.

For improved convergence of the eigenfunction expansion, it is always recommended to reduce the importance of the equation and boundary source terms, with the associated gain in computational performance [36]. Therefore, the following filtering solution for problem (4) is proposed:

$$\theta(X, Y, Z, \tau) = \theta_H(X, Y, Z, \tau) + \theta_P(X, Y, Z, \tau) \quad (7)$$

where $\theta_P(X, Y, Z)$ is the solution of the steady-state conjugated problem, which is here defined as a filtering solution, and $\theta_H(X, Y, Z, \tau)$ is the solution of the homogeneous version of the transient problem (4).

Steady state conjugated problem

With respect to the present transient problem solution, other simpler filters can be proposed, but the steady state solution is well known for having excellent characteristics for convergence acceleration of transient problems, and for this reason it has been the adopted filter. The steady state solution could have been obtained by the pseudo-transient solution path in the partial transformation scheme [55], but here a total double transformation is preferred, reaching a transformed ODEs system in the longitudinal coordinate only. The dimensionless steady conjugated problem that defines the filter is given by:

$$W(X, Y)U(X, Y) \frac{\partial \theta_P}{\partial Z} = \frac{4}{\sigma_x^2} \frac{\partial}{\partial X} \left[K(X, Y) \frac{\partial \theta_P}{\partial X} \right] + \frac{4}{\sigma_y^2} \frac{\partial}{\partial Y} \left[K(X, Y) \frac{\partial \theta_P}{\partial Y} \right] + \frac{K(X, Y)}{Pe^2} \frac{\partial^2 \theta_P}{\partial Z^2} \quad (8a)$$

$$\theta_P(0, Y, Z) = 0; \theta_P(2, Y, Z) = 0; 0 \leq Y \leq 2, 0 \leq Z \leq Z_\infty \quad (8b,c)$$

$$\theta_P(X, 0, Z) = 0; \theta_P(X, 2, Z) = 0; 0 \leq X \leq 2, 0 \leq Z \leq Z_\infty \quad (8d,e)$$

$$\theta_P(X, Y, 0) = 1; \left. \frac{\partial \theta_P}{\partial Z} \right|_{Z=Z_\infty} = 0; 0 \leq X \leq 2, 0 \leq Y \leq 2 \quad (8f,g)$$

The chosen transformation strategy for solving Eq. (8) is based on a two-dimensional eigenfunction expansion to eliminate the transversal coordinates, leading to a transformed boundary value problem

along the longitudinal coordinate, Z . The following integral transform pair is then defined:

Transform:

$$\bar{\theta}_{P_i}(Z) = \int_0^2 \int_0^2 \frac{K(X, Y)}{Pe^2} \theta_P(X, Y, Z) \tilde{\xi}_i(X, Y) dXdY \quad (9a)$$

Inverse:

$$\theta_P(X, Y, Z) = \sum_{i=1}^{\infty} \tilde{\xi}_i(X, Y) \bar{\theta}_{P_i}(Z) \quad (9b)$$

The normalized eigenfunction and its associated eigenvalues come from the following proposed eigenvalue problem:

$$\frac{4}{\sigma_x^2} \frac{\partial}{\partial X} \left[K(X, Y) \frac{\partial \xi_i}{\partial X} \right] + \frac{4}{\sigma_y^2} \frac{\partial}{\partial Y} \left[K(X, Y) \frac{\partial \xi_i}{\partial Y} \right] + \beta_i^2 \frac{K(X, Y)}{Pe^2} \xi_i(X, Y) = 0 \quad (10a)$$

$$\xi_i(0, Y) = 0; \xi_i(2, Y) = 0, 0 \leq Y \leq 2 \quad (10b,c)$$

$$\xi_i(X, 0) = 0; \xi_i(X, 2) = 0, 0 \leq X \leq 2 \quad (10d,e)$$

and the normalized eigenfunctions are calculated from:

$$\tilde{\xi}_i(X, Y) = \frac{\xi_i(X, Y)}{\sqrt{N_{\xi_i}}} \quad (10f)$$

with the normalization integrals given by:

$$N_{\xi_i} = \int_0^2 \int_0^2 \frac{K(X, Y)}{Pe^2} \xi_i(X, Y)^2 dXdY \quad (10g)$$

This eigenvalue problem with space variable coefficients can be handled by the GITT itself with the proposition of a simpler auxiliary problem, expanding the unknown eigenfunctions in terms of the chosen basis, following the procedure described in Refs. [10, 42]. Thus, a simpler auxiliary problem is defined as:

$$\frac{4}{\sigma_x^2} \frac{\partial^2 \Omega_k}{\partial X^2} + \frac{4}{\sigma_y^2} \frac{\partial^2 \Omega_k}{\partial Y^2} + \nu_k^2 \Omega_k(X, Y) = 0, 0 < X < 2, 0 < Y < 2 \quad (11a)$$

$$\Omega_k(0, Y) = 0; \Omega_k(2, Y) = 0, 0 \leq Y \leq 2 \quad (11b,c)$$

$$\Omega_k(X, 0) = 0; \Omega_k(X, 2) = 0, 0 \leq X \leq 2 \quad (11d,e)$$

Applying separation of variables to problem (11), it is found that the auxiliary eigenfunction can be expressed as a product of two one-dimensional eigenfunctions, as:

$$\Omega(X, Y) = \omega(X) \Gamma(Y) \quad (12a)$$

where,

$$\frac{4}{\sigma_x^2} \frac{d^2 \omega}{dX^2} + \nu_x^2 \omega(X) = 0 \quad (12b)$$

$$\omega(0) = 0; \omega(2) = 0 \quad (12c,d)$$

$$\frac{4}{\sigma_y^2} \frac{d^2 \Gamma}{dY^2} + \nu_y^2 \Gamma(Y) = 0 \quad (12e)$$

$$\Gamma(0) = 0; \Gamma(2) = 0 \quad (12f,g)$$

Problems (12) are readily solved in analytical form and the auxiliary eigenfunctions and eigenvalues are given by:

$$\Omega_k(X, Y) = \Omega_{m,n}(X, Y) = \sin\left(\frac{m\pi X}{2}\right) \sin\left(\frac{n\pi Y}{2}\right),$$

with $\nu_k^2 = \nu_{m,n}^2 = \nu_{x_m}^2 + \nu_{y_n}^2$

(13a,b)

Then, the following transform-inverse pair is proposed for the expansion of the original eigenfunctions, with the corresponding normalized eigenfunction and normalization integral:

Transform:

$$\bar{\xi}_{m,n}^{(i)} = \int_0^2 \int_0^2 \tilde{\Omega}_{m,n}(X, Y) \xi_i(X, Y) dXdY \quad (14a)$$

Inverse:

$$\xi_i(X, Y) = \sum_{n=1}^{\infty} \sum_{m=1}^{\infty} \tilde{\Omega}_{m,n}(X, Y) \bar{\xi}_{m,n}^{(i)} \quad (14b)$$

$$\tilde{\Omega}_{m,n}(X, Y) = \frac{\Omega_{m,n}(X, Y)}{\sqrt{N_{\Omega_{m,n}}}}, N_{\Omega_{m,n}} = \int_0^2 \int_0^2 \Omega_{m,n}(X, Y)^2 dXdY \quad (14c,d)$$

For computational purposes, it is preferable to rewrite the double summation of the inverse formula (14b) as a single summation according to an appropriate reordering rule, to account for the most relevant terms of the multiple summation in the final numerical result [39]. Since the final solution is not known a priori, the simplest proposition is the ascending order of the squared eigenvalues $\nu_{m,n}^2$ defined in Eq. (13b). Thus, for each index k is associated a pair (m, n) corresponding to the indices in the eigenvalues for each coordinate direction, as given by Eqs. (13a,b), once the eigenvalues are reorganized in ascending order [39]. Then, the inverse formula (14b) becomes:

$$\xi_i(X, Y) = \sum_{k=1}^{\infty} \tilde{\Omega}_k(X, Y) \bar{\xi}_k^{(i)} \quad (14e)$$

The integral transformation of the eigenvalue problem with space variable coefficients is then achieved by operating with $\int_0^2 \int_0^2 \tilde{\Omega}_k(X, Y) - dXdY$, and substituting

the inverse formula (14e), to obtain the following algebraic eigensystem:

$$(\mathbf{A} + \mathbf{C})\bar{\xi} = \beta^2 \mathbf{B}\bar{\xi} \quad (15a)$$

$$A_{kl} = - \int_0^2 \int_0^2 \left\{ \frac{4}{\sigma_x^2} [1 - K(X, Y)] \frac{\partial \tilde{\Omega}_k}{\partial X} \frac{\partial \tilde{\Omega}_l}{\partial X} + \frac{4}{\sigma_y^2} [1 - K(X, Y)] \frac{\partial \tilde{\Omega}_k}{\partial Y} \frac{\partial \tilde{\Omega}_l}{\partial Y} \right\} dXdY \quad (15b)$$

$$C_{kl} = \nu_k^2 \delta_{kl}; B_{kl} = \int_0^2 \int_0^2 \frac{K(X, Y)}{Pe^2} \tilde{\Omega}_k(X, Y) \tilde{\Omega}_l(X, Y) dXdY \quad (15c,d)$$

Well-established algorithms for matrix eigensystem analysis can readily solve the algebraic problem given by Eq. (15), obtaining the vector of eigenvalues β and the eigenvectors $\bar{\xi}$, after truncation to a sufficiently large finite order N_F . Then, operating the steady energy equation (8a) with $\int_0^2 \int_0^2 \tilde{\xi}_i(X, Y) - dXdY$ and making use of the inverse formula and boundary conditions, it results the following coupled system of ordinary differential equations for the steady state transformed temperatures:

$$\sum_{j=1}^{\infty} M_{ij} \frac{d\bar{\theta}_{P_i}}{dZ} = -\beta_i^2 \bar{\theta}_{P_i}(Z) + \frac{d^2 \bar{\theta}_{P_i}}{dZ^2} \quad (16a)$$

$$\bar{\theta}_{P_i}(0) = \int_0^2 \int_0^2 \frac{K(X, Y)}{Pe^2} \tilde{\xi}_i(X, Y) dXdY; \left. \frac{d\bar{\theta}_{P_i}}{dZ} \right|_{Z=Z_{\infty}} = 0 \quad (16b,c)$$

$$M_{ij} = \int_0^2 \int_0^2 W(X, Y) U(X, Y) \tilde{\xi}_i(X, Y) \tilde{\xi}_j(X, Y) dXdY \quad (16d)$$

The infinite system is then truncated to a sufficiently large order N_p and, despite being a coupled system, may be solved analytically via diagonalization of the coefficients matrix in the ODE system. Rewriting Eqs. (16a-d) as a first order ODE system, we then have:

$$\bar{\theta}_{P_{i+N_p}}(Z) = \frac{d\bar{\theta}_{P_i}}{dZ}; \sum_{j=1}^{N_p} M_{ij} \bar{\theta}_{P_{j+N_p}}(Z) = -\beta_i^2 \bar{\theta}_{P_i}(Z) + \frac{d\bar{\theta}_{P_{i+N_p}}}{dZ} \quad (16e,f)$$

$$\bar{\theta}_{P_i}(0) = \int_0^2 \int_0^2 \frac{K(X, Y)}{Pe^2} \tilde{\xi}_i(X, Y) dXdY; \left. \frac{d\bar{\theta}_{P_i}}{dZ} \right|_{Z=Z_{\infty}} = 0 \quad (16g,h)$$

or in matrix form,

$$\boldsymbol{\varphi}' + \mathbf{L}\boldsymbol{\varphi} = 0 \quad (17a)$$

where \mathbf{L} is the coefficients matrix of order $2N_p$, independent of the axial coordinate, and the solution vector is formed by:

$$\boldsymbol{\varphi} = \left\{ \bar{\theta}_{P_1}(Z), \dots, \bar{\theta}_{P_{N_p}}(Z), \frac{d\bar{\theta}_{P_{N_p+1}}}{dZ}, \dots, \frac{d\bar{\theta}_{P_{2N_p}}}{dZ} \right\}^T \quad (17b)$$

The corresponding matrix eigensystem problem for solving Eq. (17a) is then given by:

$$(\mathbf{L} - \alpha \mathbf{I})\boldsymbol{\zeta} = 0 \quad (18)$$

where \mathbf{I} is the identity matrix, α are the eigenvalues of the matrix \mathbf{L} , and $\boldsymbol{\zeta}$ are the associated eigenvectors. The solution for the transformed potentials and their derivatives is then constructed as:

$$\varphi_i(Z) = \sum_{j=1}^{2N_p} c_j \zeta_{i,j} e^{-\alpha_j Z}, \quad i = 1, \dots, 2N_p \quad (19a)$$

where the constants c_j are obtained so as to satisfy the boundary conditions, yielding the following linear algebraic system:

$$c_1 \zeta_{i,1} + \dots + c_{2N_p} \zeta_{i,2N_p} = \int_0^2 \int_0^2 \frac{K(X,Y)}{Pe^2} \tilde{\zeta}_i(X,Y) dXdY, \quad i = 1, \dots, N_p \quad (19b)$$

$$c_1 \zeta_{i,1} e^{-\alpha_1 Z_\infty} + \dots + c_{2N_p} \zeta_{i,2N_p} e^{-\alpha_{2N_p} Z_\infty} = 0, \quad i = N_p + 1, \dots, 2N_p \quad (19c)$$

Once the constants c_j are obtained from the numerical solution of system (19), the solution vector is reconstructed from Eq. (19a). The inverse formula of the steady conjugated problem, Eq. (9b), is then recalled obtaining the dimensionless temperature at any (X, Y, Z) position, yielding the desired solution of the filter problem, and the steady state solution of the original problem itself.

Homogeneous transient conjugated problem

The homogeneous counterpart of the transient conjugated problem, after substituting the filtering proposal stated in Eq. (7) and the filter problem, Eq. (8), becomes the following partial differential equation:

$$\begin{aligned} W(X, Y) \left[\frac{\partial \theta_H}{\partial \tau} + U(X, Y) \frac{\partial \theta_H}{\partial Z} \right] \\ = \frac{4}{\sigma_x^2} \frac{\partial}{\partial X} \left[K(X, Y) \frac{\partial \theta_H}{\partial X} \right] + \frac{4}{\sigma_y^2} \frac{\partial}{\partial Y} \left[K(X, Y) \frac{\partial \theta_H}{\partial Y} \right] \\ + \frac{1}{Pe^2} \frac{\partial}{\partial Z} \left[K(X, Y) \frac{\partial \theta_H}{\partial Z} \right], \end{aligned} \quad (20a)$$

$$0 < X < 2, 0 < Y < 2, 0 < Z < Z_\infty, \tau > 0 \quad (20a)$$

$$\theta_H(0, Y, Z, \tau) = 0, \theta_H(2, Y, Z, \tau) = 0, 0 \leq Y \leq 2, 0 \leq Z \leq Z_\infty, \tau > 0 \quad (20b,c)$$

$$\theta_H(X, 0, Z, \tau) = 0, \theta_H(X, 2, Z, \tau) = 0, 0 \leq X \leq 2, 0 \leq Z \leq Z_\infty, \tau > 0 \quad (20d,e)$$

$$\theta_H(X, Y, 0, \tau) = 0, \left. \frac{\partial \theta_H}{\partial Z} \right|_{Z=Z_\infty} = 0, 0 \leq X \leq 2, 0 \leq Y \leq 2, \tau > 0 \quad (20f,g)$$

$$\theta_H(X, Y, Z, 0) = 1 - \theta_p(X, Y, Z), 0 \leq X \leq 2, 0 \leq Y \leq 2, 0 \leq Z \leq Z_\infty \quad (20h)$$

In order to solve the homogeneous transient problem through integral transformation, the following transform-inverse pair is defined:

Transform:

$$\bar{\theta}_{H_i}(\tau) = \int_0^{Z_\infty} \int_0^2 \int_0^2 W(X, Y) \theta_H(X, Y, Z, \tau) \tilde{\Psi}_i(X, Y, Z) dXdYdZ \quad (21a)$$

Inverse:

$$\theta_H(X, Y, Z, \tau) = \sum_{i=1}^{\infty} \tilde{\Psi}_i(X, Y, Z) \bar{\theta}_{H_i}(\tau) \quad (21b)$$

The normalized eigenfunctions and the associated eigenvalues come from solving the following three-dimensional eigenvalue problem:

$$\begin{aligned} \frac{4}{\sigma_x^2} \frac{\partial}{\partial X} \left[K(X, Y) \frac{\partial \Psi_i}{\partial X} \right] + \frac{4}{\sigma_y^2} \frac{\partial}{\partial Y} \left[K(X, Y) \frac{\partial \Psi_i}{\partial Y} \right] \\ + \frac{1}{Pe^2} \frac{\partial}{\partial Z} \left[K(X, Y) \frac{\partial \Psi_i}{\partial Z} \right] \\ + \mu_i^2 W(X, Y) \Psi_i(X, Y, Z) = 0 \end{aligned} \quad (22a)$$

$$\Psi_i(0, Y, Z) = 0, \Psi_i(2, Y, Z) = 0, 0 \leq Y \leq 2, 0 \leq Z \leq Z_\infty \quad (22b,c)$$

$$\Psi_i(X, 0, Z) = 0, \Psi_i(X, 2, Z) = 0, 0 \leq X \leq 2, 0 \leq Z \leq Z_\infty \quad (22d,e)$$

$$\Psi_i(X, Y, 0) = 0, \left. \frac{\partial \Psi_i}{\partial Z} \right|_{Z=Z_\infty} = 0, 0 \leq X \leq 2, 0 \leq Y \leq 2 \quad (22f,g)$$

and the normalized eigenfunctions with the normalization integrals are calculated from:

$$\tilde{\Psi}_i(X, Y, Z) = \frac{\Psi_i(X, Y, Z)}{\sqrt{N_{\Psi_i}}}; N_{\Psi_i} = \int_0^{Z_\infty} \int_0^2 \int_0^2 W(X, Y) \Psi_i(X, Y, Z)^2 dXdYdZ \quad (22h,i)$$

As previously stated, the eigenvalue problem with space variable coefficients defined in Eq. (22) can be handled by the GITT itself with the proposition of a simpler auxiliary problem. Hence, the following auxiliary eigenvalue problem has been chosen:

$$\frac{4}{\sigma_x^2} \frac{\partial^2 \chi_k}{\partial X^2} + \frac{4}{\sigma_y^2} \frac{\partial^2 \chi_k}{\partial Y^2} + \frac{1}{Pe^2} \frac{\partial^2 \chi_k}{\partial Z^2} + \lambda_k^2 \chi_k = 0; 0 < X < 2, 0 < Y < 2, 0 < Z < Z_\infty \quad (23a)$$

$$\chi_k(0, Y, Z) = 0, \chi_k(2, Y, Z) = 0, 0 \leq Y \leq 2, 0 \leq Z \leq Z_\infty \quad (23b,c)$$

$$\chi_k(X, 0, Z) = 0, \chi_k(X, 2, Z) = 0, 0 \leq X \leq 2, 0 \leq Z \leq Z_\infty \quad (23d,e)$$

$$\chi_k(X, Y, 0) = 0, \left. \frac{\partial \chi_k}{\partial Z} \right|_{Z=Z_\infty} = 0, 0 \leq X \leq 2, 0 \leq Y \leq 2 \quad (23f, g)$$

As in the previous section, one can solve problem (23) via separation of variables, then employ a reordering scheme to rewrite the triple summation as a single one; each index then corresponds to the position of the triad of eigenvalues associated with each direction when sorted in ascending order of the sum of their squares. Thus, the following transform-inverse pair is proposed for the expansion of the original eigenfunctions:

Transform:

$$\bar{\Psi}_k^{(i)} = \int_0^{Z_\infty} \int_0^2 \int_0^2 \tilde{\chi}_k(X, Y, Z) \Psi_i(X, Y, Z) dXdYdZ \quad (24a)$$

Inverse:

$$\Psi_i(X, Y, Z) = \sum_{k=1}^{\infty} \tilde{\chi}_k(X, Y, Z) \bar{\Psi}_k^{(i)} \quad (24b)$$

where the normalized eigenfunctions and normalization integrals are given by the following expression:

$$\tilde{\chi}_k(X, Y, Z) = \frac{\chi_k(X, Y, Z)}{\sqrt{N_{\chi_k}}}, \quad (24c, d)$$

$$N_{\chi_k} = \int_0^{Z_\infty} \int_0^2 \int_0^2 \chi_k(X, Y, Z)^2 dXdYdZ$$

The integral transformation of the differential eigenvalue problem with space variable coefficients, Eqs. (22a–g), is then achieved by operating with $\int_0^{Z_\infty} \int_0^2 \int_0^2 \tilde{\chi}_l(X, Y, Z) - dXdYdZ$, yielding the following algebraic eigensystem:

$$(\mathbf{D} + \mathbf{E})\bar{\Psi} = \mu^2 F \bar{\Psi} \quad (25a)$$

$$D_{kl} = - \int_0^{Z_\infty} \int_0^2 \int_0^2 [1 - K(X, Y)] \left\{ \frac{4}{\sigma_x^2} \frac{\partial \tilde{\chi}_k}{\partial X} \frac{\partial \tilde{\chi}_l}{\partial X} + \frac{4}{\sigma_y^2} \frac{\partial \tilde{\chi}_k}{\partial Y} \frac{\partial \tilde{\chi}_l}{\partial Y} + \frac{1}{Pe^2} \frac{\partial \tilde{\chi}_k}{\partial Z} \frac{\partial \tilde{\chi}_l}{\partial Z} \right\} dXdYdZ \quad (25b)$$

$$E_{kl} = \lambda_k^2 \delta_{kl}; F_{kl} = \int_0^{Z_\infty} \int_0^2 \int_0^2 W(X, Y) \tilde{\chi}_k(X, Y, Z) \tilde{\chi}_l(X, Y, Z) dXdYdZ \quad (25c, d)$$

As previously discussed, well-established algorithms for matrix eigensystem analysis can be recalled to numerically solve the algebraic problem given by Eq. (25), yielding the eigenvalues μ and the eigenvectors $\bar{\Psi}$, after truncation to a large finite order N_H sufficient to warrant convergence to a desired accuracy target. Then, operating the homogeneous transient energy equation (20a) with $\int_0^{Z_\infty} \int_0^2 \int_0^2 \tilde{\Psi}_i(X, Y, Z) - dXdYdZ$ and making use of the original eigenvalue

problem equation, Eqs. (22a–g), and the inverse formula (21b), one obtains the following initial value problem of ordinary differential equations for the homogeneous transient transformed temperatures:

$$\frac{d\bar{\theta}_{H_i}}{d\tau} + \mu_i^2 \bar{\theta}_{H_i}(\tau) + \sum_{j=1}^{\infty} \bar{G}_{i,j} \bar{\theta}_{H_j}(\tau) = 0, i = 1, 2, 3, \dots \quad (26a)$$

$$\bar{G}_{i,j} = \int_0^{Z_\infty} \int_0^2 \int_0^2 W(X, Y) U(X, Y) \tilde{\Psi}_i(X, Y, Z) \frac{\partial \tilde{\Psi}_j}{\partial Z} dXdYdZ \quad (26b)$$

with the transformed initial conditions:

$$\bar{\theta}_{H_i}(0) = \bar{f}_i = \int_0^{Z_\infty} \int_0^2 \int_0^2 W(X, Y) [1 - \theta_p(X, Y, Z)] \tilde{\Psi}_i(X, Y, Z) dXdYdZ \quad (26c)$$

The infinite system is truncated to a sufficiently large order N_T for the desired precision target and, again, the transformed system of equations (26a–c), despite being coupled, is linear and has analytical solution through the appropriate matrix eigensystem analysis. For this purpose, it is written in matrix form as:

$$\bar{\theta}'_H(\tau) + \mathbf{G} \bar{\theta}_H(\tau) = 0; \bar{\theta}_H(0) = \bar{\mathbf{f}} \quad (27a, b)$$

where \mathbf{G} , the coefficients matrix independent from the time variable, and the transformed initial conditions vector, $\bar{\mathbf{f}}$, are given by:

$$\mathbf{G} = \left\{ \mu_i^2 \delta_{i,j} + \bar{G}_{i,j} \right\}_{i,j=1,2,3,\dots}; \bar{\mathbf{f}} = \left\{ \bar{f}_i \right\}_{i=1,2,3,\dots} \quad (27c, d)$$

The solution for the transformed temperatures vector is then conveniently written in terms of the matrix exponential function as:

$$\bar{\theta}_H(\tau) = \exp(-\mathbf{G}\tau) \cdot \bar{\mathbf{f}} \quad (28)$$

The inversion formula of the homogeneous transient conjugated problem, Eq. (21b), is then recalled, together with the filter proposal, Eq. (7), to provide the dimensionless temperature field for any dimensionless position and time, (X, Y, Z, τ) , leading to the desired solution of the transient three-dimensional conjugated problem. Once the temperature distribution has been derived, the transient bulk temperature along the channel length is given from its definition as:

$$\theta_{av}(Z, \tau) = \frac{\int_A \theta(X, Y, Z, \tau) U(X, Y) dA}{\int_A U(X, Y) dA} \quad (29)$$

Table 1. Thermophysical properties of the working fluid and substrates.

Thermophysical Properties at 20 °C			
	ρ (kg/m ³)	c_p (kJ/kg K)	k (W/m K)
Water	998	3.18	0.60
PDMS	970	1.46	0.15
Fused Silica	2220	0.74	1.38
Commercial Copper (90% Cu, 10% Al)	8800	0.42	52

Table 2. Geometric parameters for the test case of a square channel ($AR = 1$).

Parameter	Value	Parameter	Value
L_{xM}	100 μm	D_h	100 μm
L_{yM}	100 μm	σ_x	2
L_{xT}	200 μm	σ_y	2
L_{yT}	200 μm	Pe	1

Table 3. Convergence of the first ten eigenvalues of the two-dimensional eigenvalue problem in the case of a square channel ($AR = 1$).

B	$N_F=200$	$N_F=400$	$N_F=600$	$N_F=800$	$N_F=1000$
1	1.4208	1.4162	1.4147	1.4136	1.4128
2	3.3352	3.3345	3.3341	3.3339	3.3338
3	3.3352	3.3345	3.3341	3.3339	3.3338
4	4.4429	4.4429	4.4429	4.4429	4.4429
5	5.3523	5.3380	5.3336	5.3303	5.3278
6	5.5828	5.5720	5.5686	5.5662	5.5643
7	5.9380	5.9263	5.9206	5.9176	5.9153
8	5.9380	5.9263	5.9206	5.9176	5.9153
9	6.6181	6.5938	6.5772	6.5705	6.5653
10	6.6181	6.5938	6.5772	6.5705	6.5653

Results and discussion

Convergence analysis and verification

The fully developed velocity profile is taken from well-known exact analytical solutions [36], as presented in Eqs. (6a–f). For this reason, the focus of the work is directed toward analyzing the temperature field and other derived quantities, in order to probe the adequacy of the integral transforms approach here proposed.

In order to identify typical values of the dimensionless governing parameters, one fluid and three substrate materials were selected from previous experiments, as shown in Table 1, with water as working fluid and PDMS (polydimethylsiloxane), Fused Silica and Commercial Copper (90% Cu, 10% Al) as substrates, first of all seeking comparisons with the analysis presented in Ref. [55]. The chosen geometric parameters for a square channel, which are employed to characterize the dimensionless parameters, are presented in Table 2. The results that follow encompass temperature profiles in the transient and steady regimen for the cases of the squared cross section ($AR = 1$) and rectangular channels with different wall thicknesses, for fixed channel width and variable channel height.

Table 4. Convergence of the first ten eigenvalues of the three-dimensional eigenvalue problem in the case of a square channel ($AR = 1$).

μ	$N_H=200$	$N_H=400$	$N_H=600$	$N_H=800$	$N_H=1000$
1	1.4482	1.4330	1.4323	1.4317	1.4314
2	1.6878	1.6746	1.6740	1.6735	1.6732
3	2.0856	2.0747	2.0743	2.0739	2.0737
4	2.5681	2.5597	2.5594	2.5591	2.5590
5	3.0957	3.0948	3.0891	3.0889	3.0889
6	3.1948	3.1939	3.1919	3.1919	3.1918
7	3.1948	3.1939	3.1919	3.1919	3.1918
8	3.3044	3.3033	3.3014	3.3014	3.3014
9	3.3044	3.3033	3.3014	3.3014	3.3014
10	3.5130	3.5117	3.5100	3.5100	3.5099

Table 5. Convergence of the dimensionless temperature profile for the case of the squared channel ($AR = 1$), at the centerline ($X = 1$ and $Y = 1$) of the microfluidic apparatus.

$\tau = 0.5$							
N_T	$Z = 0.1$	$Z = 0.2$	$Z = 0.3$	$Z = 0.5$	$Z = 0.75$	$Z = 1$	$Z = 2$
30	0.9591	0.9182	0.8709	0.7766	0.6764	0.6031	0.4908
60	0.9585	0.9171	0.8695	0.7754	0.6761	0.6032	0.4914
90	0.9578	0.9157	0.8675	0.7725	0.6722	0.5980	0.4820
120	0.9575	0.9153	0.8671	0.7725	0.6725	0.5981	0.4820
150	0.9567	0.9137	0.8648	0.7690	0.6672	0.5905	0.4665
180	0.9567	0.9136	0.8649	0.7693	0.6675	0.5905	0.4665
COMSOL	0.9596	0.9144	0.8668	0.7739	0.6745	0.6006	0.4889
Rel. Deviation (%)	0.31	0.08	0.18	0.47	0.9	1.5	4.1

In order to analyze the convergence of the eigenfunction expansions for the temperature distribution, one needs first to evaluate the convergence of the two and three-dimensional eigenvalue problems solutions, based on the integral transformation with simpler auxiliary eigenvalue problems. Thus, Tables 3 and 4 illustrate the convergence of the 2D and 3D eigenvalue problems in the case of a square channel. The presented first ten eigenvalues converge to at least the third significant digit with truncation orders as low as N_F or $N_H=1000$, where it is noticed a slower convergence rate, as expected, relative to the two-dimensional eigenvalue problem in Ref. [55], given that the symmetry of the problem has been accounted for beforehand in that work, thus reducing the number of terms required for convergence. The convergence behavior of the eigenvalue problems expansions can be enhanced by employing, for instance, an extended integral balance approach for Sturm-Liouville problems [67].

Table 5 offers a brief convergence analysis of the transient dimensionless temperature at the centerline ($X = 1$ and $Y = 1$) and time $\tau = 0.5$, for selected values of the axial coordinate. The centerline dimensionless temperature is converged to ± 1 in the fourth significant digit, for truncation orders up to $N_T=180$ terms. Also shown are the results from the commercial software

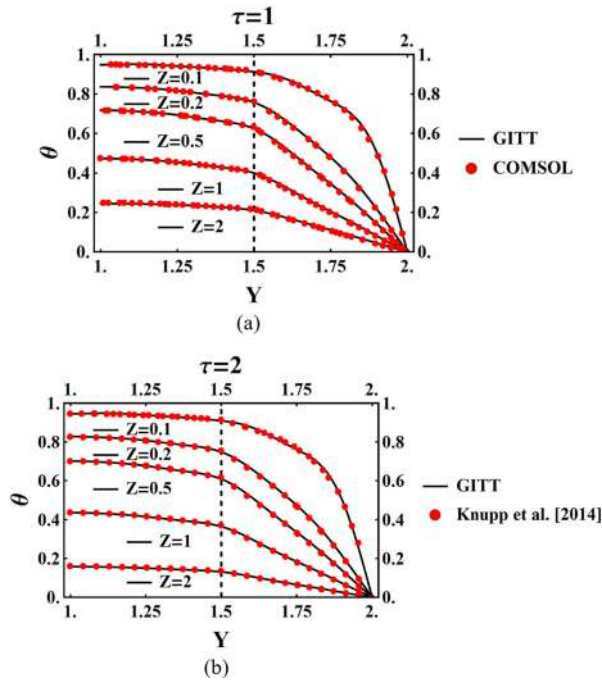


Figure 2. Dimensionless temperature profiles in transient state for a squared channel: (a) at $\tau = 1$, compared with COMSOL solution and (b) At steady state ($\tau = 2$) compared with the GITT solution with partial transformation scheme [55], across the transversal coordinate, $Y \in [1, 2]$, at the central plane ($X = 1$) and for different axial positions.

COMSOL Multiphysics® finite element method simulation, with corresponding relative deviations.

Figure 2a,b shows the dimensionless temperature profiles in a square channel with water as working fluid and PDMS as substrate, across the transversal coordinate, $Y = 1$ to 2, at the central plane $X = 1$, and for different times ($\tau = 1$ and 2), where the steady state is approximately represented by the larger time value ($\tau = 2$). Different axial positions along the microchannel length are plotted, where it is possible to clearly distinguish the transition at the fluid/solid interface, identified by a dashed line to highlight the position of the interface. The GITT solution at $\tau = 1$ is verified against the solution of the commercial software COMSOL Multiphysics®, whereas the solution at $\tau = 2$ is verified against the steady state GITT solution with partial transformation of Knupp et al. [55], both represented as red circles, showing excellent agreement to the graph scale in both cases.

Figure 3 shows the dimensionless temperature time evolution at the centerline of the microfluidic apparatus ($Y = 1$ and $X = 1$), located within the fluid domain, and compared with the COMSOL Multiphysics® results. Clearly, the GITT not only predicts well the spatial behavior of the micro-device, but also its temporal behavior, with only $N_T=180$ terms, which is a

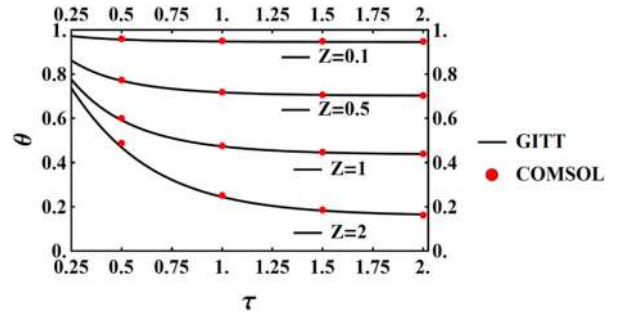


Figure 3. Dimensionless temperature profiles in transient state for a water/PDMS squared channel at its centerline ($Y = 1$ and $X = 1$), compared with COMSOL solution for different axial positions.

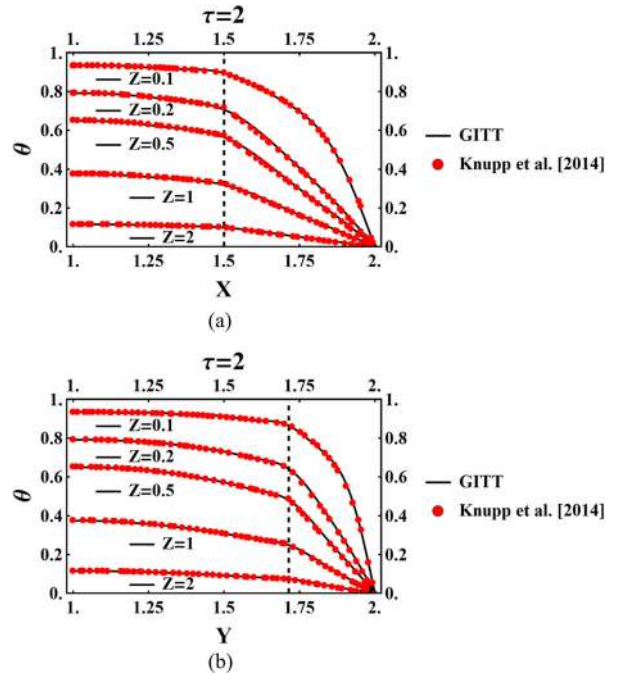


Figure 4. Dimensionless temperature profiles at steady state for a rectangular channel with aspect ratio $AR = 1.42$, compared against the GITT solution with partial transformation of Knupp et al. [55]: (a) along the width of the microfluidic apparatus, at the center plane ($Y = 1$) and (b) along the height of the micro-device, at the center plane ($X = 1$), for different axial positions.

fairly low truncation order for the eigenfunction expansion, given the complexity of the problem (three-dimensional transient conjugated formulation).

Figure 4 shows the steady state ($\tau = 2$) dimensionless temperature profiles for a rectangular channel with aspect ratio $AR = 1.42$, again across the transversal coordinate, $Y = 1$ to 2, at the central plane $X = 1$ of the channel-substrate arrangement, for different longitudinal positions. Following Knupp et al. [55], the width of the channel is fixed while the height is varied with respect to the square channel case. The

Table 6. Materials and conductivities ratio considered in the present work.

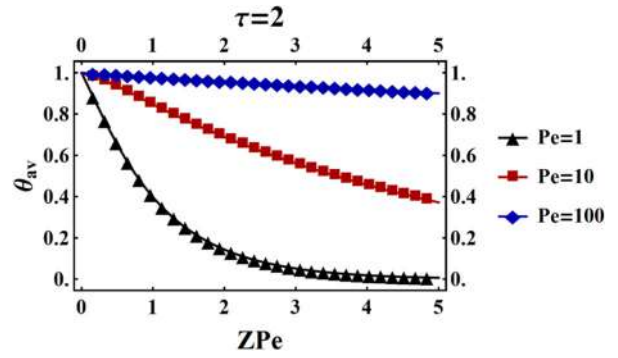
Thermal conductivities ratio	
Materials	k_s/k_f
PDMS/Water	0.25
Silica/Water	2.3
Copper/Water	86.66

Table 7. Maximum dimensionless temperature variation across the channel.

$\Delta\theta_{cw}$			
Materials	$Z = 0.5$	$Z = 1$	$Z = 1.5$
PDMS/Water	0.110	0.086	0.053
Silica/Water	0.066	0.031	0.010
Copper/Water	0.025	0.008	0.001

present GITT solution obtained with the total transformation scheme has an excellent agreement with the GITT solution obtained by Knupp et al. [55] with the pseudo-transient formulation and the partial transformation scheme, when a two-dimensional eigenvalue problem was adopted and a partial differential system for the transformed temperatures, with time and longitudinal coordinate as independent variables, is numerically solved for. The proposed total transformation scheme, with its transformed problem consisting of a system of ordinary differential equations solvable by the associated matrix eigensystem analysis, bears a noticeable advantage when compared with the transformed partial differential equations system stemming from the partial transformation alternative strategy adopted in Ref. [55], both in terms of computational cost and numerical accuracy. A more complete comparative analysis of the total and partial transformation schemes in multidimensional convection-diffusion problems was provided in Ref. [68]. The adherence of these results confirms not only the robustness of the integral transform approach, but also its flexibility in terms of solution path choices.

Table 6 provides the values of the thermal conductivity ratio, an important parameter in conjugated heat transfer, for the three different substrates cases here considered. Table 7 shows the maximum dimensionless temperature variation across the wall, $\Delta\theta_{cw}$, for the three cases and at three different longitudinal positions, which shows that, as expected, there is a more marked temperature variation across the height of the channel closer to the channel entry ($Z = 0.5$) and for smaller thermal conductivity ratio. The higher thermal conductivities ratio, for fixed Peclet number and aspect ratio, increases the conjugation parameter as defined in Refs. [29, 46] and favors the adoption of the approximate lumped-differential model that lumps

**Figure 5.** Dimensionless bulk temperature along the scaled dimensionless axial coordinate for different Peclet numbers, with $AR = 1$ and $\tau = 2$.

the temperature distribution in the transversal direction at the wall, due to the milder transversal temperature gradients, and accounts for axial conduction only in the solid region.

Figure 5 illustrates the effect of Peclet number on the dimensionless bulk temperature distribution at the fluid region of the microfluidic apparatus, across the scaled axial coordinate ZPe , for $AR = 1$, again with the fluid/solid combination of water/PDMS. For lower Pe numbers, the increased relevance of fluid axial conduction alters the usual proportionality between thermal entry length and hydraulic diameter ratio with the Peclet number. Nevertheless, the conjugation effect does not alter the same qualitative behavior, i.e., larger thermal entry lengths with rising Pe , as can be extracted from the comparison of the curves for $Pe = 1$ to 100 in Figure 5, which stems from the lower residence times of the fluid within the channel offsetting the wall participation in heat transfer.

Figure 6 shows the dimensionless fluid bulk temperature at steady state along the axial coordinate, now varying the aspect ratio AR for a fixed $Pe = 1$, again utilizing water as working fluid and PDMS as substrate. It can be observed the more effective cooling with the reduction of the aspect ratio, while maintaining the total fluid-solid interface area.

Figure 7 depicts dimensionless temperature contours at the midplane parallel to YZ for four different values of aspect ratio, defined as the ratio between the height and the width of the channel. For an increase in aspect ratio, the wall thickness becomes smaller which is observable in Figure 7 by recognizing the purple horizontal line as the interface between the fluid and the solid. Close to the channel entrance section, the temperature assumes its highest values, as imposed by the boundary condition at $Z = 0$, both at the fluid and the wall; as the flow advances along the channel, the temperature rapidly decays as the flow

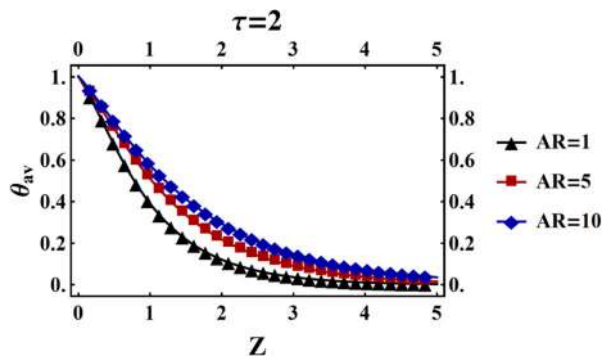


Figure 6. Dimensionless fluid bulk temperature along the axial coordinate for different aspect ratio, AR , for the same total area of the fluid-solid interface.

approaches full thermal development. Along the Y axis, the temperature decreases monotonically from the center of the channel to the edge of the solid wall. One may observe the transitions from the fluid to the solid regions, in accordance with the interface continuity conditions. The single domain formulation allows for the representation of the full region temperature distribution through a single eigenfunction expansion, which is indeed a major advantage of this solution path and permits envisioning the extension of this approach to more involved geometries and complex configurations. Besides, this precise and cost-effective simulation path is particularly handy in

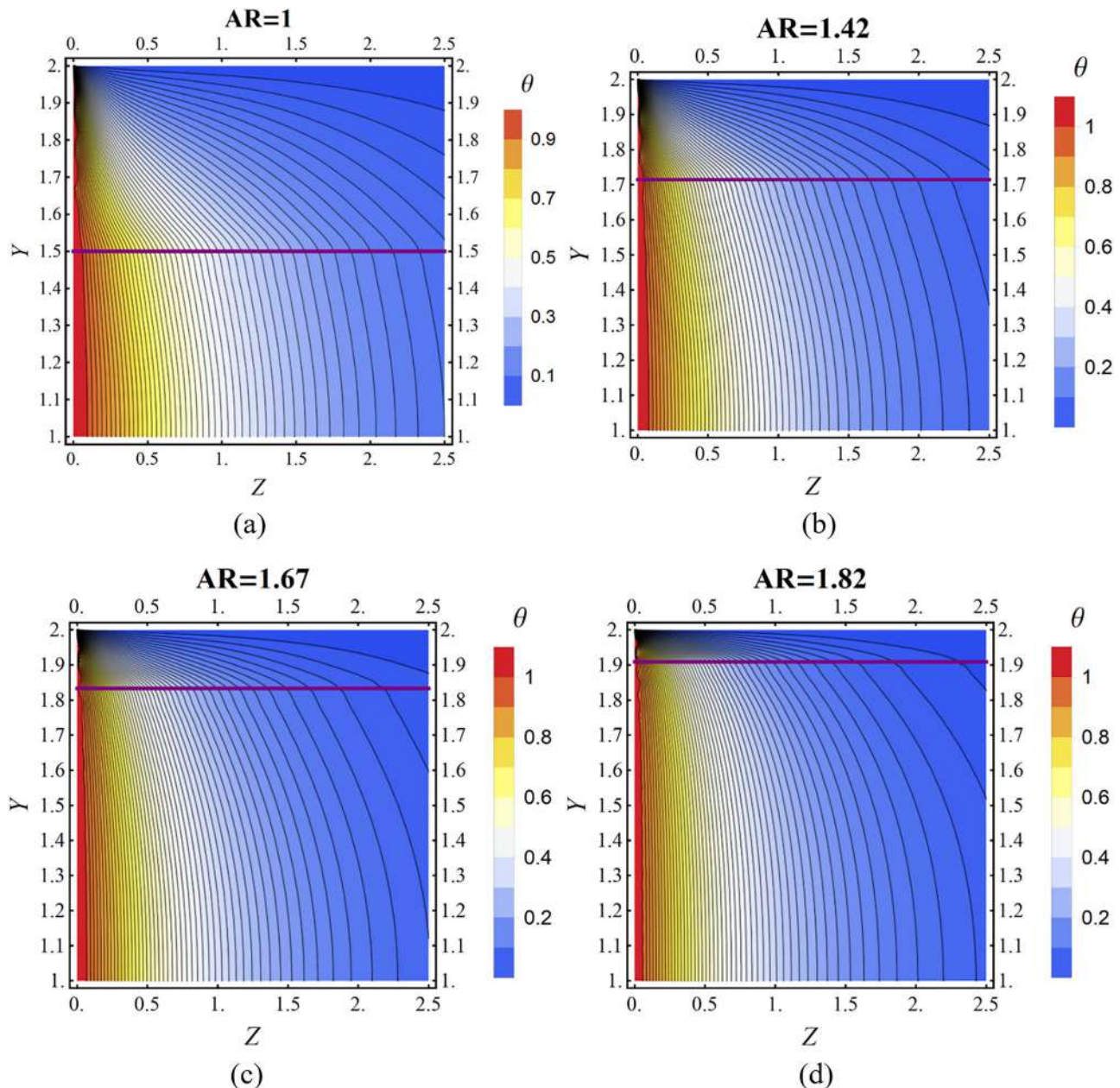


Figure 7. Dimensionless temperature contours along the axial coordinate and across the width of the microsystem, at the center plane ($X = 1$): (a) $AR = 1$, (b) $AR = 1.42$, (c) $AR = 1.67$ and (d) $AR = 1.82$.

intensive computational tasks such as inverse problem analysis of heterogeneous media, especially under the integral transformation of experimental data, as demonstrated in Refs. [69, 70].

Conclusions

The present work has analyzed transient three-dimensional conjugated heat transfer for internal laminar flow in fluidic devices based on microchannels. The proposed hybrid solution was constructed by the GITT, reformulating the problem in a single domain for the fluid current and solid substrate present on the original formulation, which are represented through space variable thermophysical properties and velocity fields, and considering both transversal and axial diffusion effects at both the wall and fluid subdomains. The spatially variable coefficients of the single domain formulation are carried on to a two-dimensional eigenvalue problem for the steady state solution, and to a three-dimensional eigenvalue problem for the transient solution, which give the basis of the corresponding eigenfunction expansions and are also solved via GITT. The results for a single rectangular microchannel show excellent agreement both on the transient regime against the results obtained by the commercial platform COMSOL, and on the steady regime with the solution obtained by Knupp et al. [55], also handled by GITT, in which the authors utilized a partial transformation scheme and a pseudo-transient formulation. The present analysis also inspected for the influence on the conjugated heat transfer behavior of parameters such as thermal conductivity ratio, aspect ratio, and Peclet number. The present contribution closes a gap on the integral transform treatment of conjugated heat transfer problems, by dealing with a fairly general transient three-dimensional situation, but also opens avenues for extensions in terms of channel transversal and longitudinal geometries, micro-device multichannel configuration, flow and thermal regimen, and micro-heat transfer scaling effects.

Acknowledgments

This paper is an extended version of a contribution to the CHT-21 - ICHMT International Symposium on Advances in Computational Heat Transfer, Paper # CHT-21-120, by the same authors, held remotely from August 15th – 19th, 2021, Rio de Janeiro, Brazil

Funding

The authors are grateful for the financial support offered by the Brazilian Government agencies CNPq, CAPES (PROCAD-Defesa), FAPERJ, and ANP/Petrogal Brasil.

Notes on contributors



Adam Hugo Reis Sousa received his B.Sc. in Chemical Engineering from the Federal University of Pará (UFPA) in 2018 and the M.Sc. in Mechanical Engineering (2021) from the Mechanical Engineering Dept. of COPPE/UFRJ, Federal University of Rio de Janeiro (UFRJ), both in Brazil. He works in the areas of conjugated prob-

lems and heat transfer at the micro-scale. In his M.Sc. dissertation he employed the Generalized Integral Transform Technique combined to the single domain formulation strategy in order to solve multidimensional conjugated heat transfer problems. He has interest in the general areas of heat and mass transfer, fluid mechanics, and thermodynamics.



Kleber Marques Lisboa received his B.Sc. in Mechanical Engineering from the Federal University of Rio de Janeiro (UFRJ), and M.Sc. and Ph.D. in Mechanical Engineering from COPPE/UFRJ, after a period as visiting scholar at the Eidgenössische Technische Hochschule Zürich (ETH Zürich), Switzerland. He was a research

assistant at IBM Zurich Research Laboratory for a year, where he has worked on the research of energy efficiency in the new generation data centers. He has received the awards ABCM/Embraer for the best Bachelor thesis in 2013, Hartnett-Irvine in 2016 given by the International Center for Heat and Mass Transfer (ICHMT), and Rien van Genuchten Early-Career Award of Porous Media for a Green World 2021 given by the International Society for Porous Media (InterPore). He is an Assistant Professor at Universidade Federal Fluminense (UFF), Brazil. He has experience in fluid mechanics and transport phenomena, majorly in the following subjects: hybrid numerical-analytical methods, transport phenomena at the microscale, heat transfer, electrochemical reactors, and phase change.



Carolina Palma Naveira Cotta is an Associate Professor of Mechanical Engineering and Head of the Nano & Microfluidics and Microsystems Lab, at COPPE/UFRJ, Federal University of Rio de Janeiro (UFRJ), Brazil, since 2011. She teaches heat transfer, mathematical meth-

ods, and transport phenomena at the nano and micro-scales. She holds the BSc (2004), MSc (2006), DSc (2009) degrees in Mechanical Engineering from UFRJ, and spent one year (2017-2018) as Visiting Professor at the Mech. Eng. Dept. of the University College London (UCL), UK. She was elected member of the Scientific Council of the International Center for Heat and Mass Transfer, ICHMT, in 2016. In 2014, she was elected Affiliate Member of the Brazilian Academy of Sciences-ABC, for the term 2015-2019, and in 2020 was elected as Affiliate Member of the World Academy of Sciences (TWAS), Italy, for the term

2021-2026. She holds competitive research productivity grants from both the federal (CNPq) and state (FAPERJ) sponsoring agencies. Her research interests are in transport phenomena at micro- and nano-scales, mainly on thermal microsystems, heat transfer enhancement, inverse problems, hybrid methods, water desalination, and sustainable energies. She also has experience in joint research with the industrial sector, including sponsored projects with major companies such as Petrobras, General Electric, INB, Shell, and GALP.



Renato Machado Cotta holds a degree in Mechanical Engineering with Nuclear Specialization from the Federal University of Rio de Janeiro (1981) and a Ph.D. degree in Mechanical & Aerospace Engineering from North Carolina State University, USA (1985). Full Professor of the Polytechnic School and COPPE, Federal University of Rio de Janeiro. Served as President of the National Nuclear Energy Commission (CNEN), Ministry of Science and Technology, Brazil, 2015-2017, and from 2020-2022 was Member of the National Council for Energy Policy, Ministry of Mines and Energy. Full Member of the Brazilian Academy of Sciences (ABC), National Academy of Engineering (ANE), and The World Academy of Sciences (TWAS). Doctor Honoris Causa, Université de Reims Champagne-Ardenne, France, and recipient of the Fellowship Award of the International Center for Heat and Mass Transfer. Served as Chairman of the Executive Committee of the International Center for Heat and Mass Transfer (ICHMT), 2016-2018, and as President of the Brazilian Association of Mechanical Sciences and Engineering, ABCM, 2000-2001. Awardee of the Medals and Memberships of the National Order of Naval Merit and of the National Order of Scientific Merit, Brazil. He works in the area of heat and mass transfer, mainly on hybrid methods in simulation, transport phenomena in the micro- and nano-scales, heat transfer enhancement, nuclear technology, and environmental contaminants dispersion. Developed technological projects with various governmental agencies and companies related to his research interests. Adjunct Professor of the University of Miami, FL, from 1993 to 2005. Leverhulme Trust Visiting Professor at the Mechanical Eng. Dept., University College London, UCL, UK (2018). Presently commissioned at AMAZUL state company, Amazônia Azul Defense Technologies, as Senior Technical Counselor for the General Director of Nuclear and Technological Development of the Brazilian Navy, Ministry of Defense.

ORCID

Kleber M. Lisboa  <http://orcid.org/0000-0003-0736-5996>
 Carolina P. Naveira-Cotta  <http://orcid.org/0000-0001-8073-5602>
 Renato M. Cotta  <http://orcid.org/0000-0003-0965-0811>

References

- [1] T. L. Perelman, "On conjugated problems of heat transfer," *Int. J. Heat Mass Transfer*, vol. 3, no. 4, pp. 293–303, 1961. DOI: [10.1016/0017-9310\(61\)90044-8](https://doi.org/10.1016/0017-9310(61)90044-8).
- [2] A. V. Luikov, V. A. Aleksashenko and A. A. Aleksashenko, "Analytical methods of solution of conjugated problems in convective heat transfer," *Int. J. Heat Mass Transfer*, vol. 14, no. 8, pp. 1047–1056, 1971. DOI: [10.1016/0017-9310\(71\)90203-1](https://doi.org/10.1016/0017-9310(71)90203-1).
- [3] P. Tabeling, *Introduction to Microfluidics*. New York, NY: Oxford University Press, 2005.
- [4] N. T. Nguyen and S. T. Wereley, *Fundamentals and Applications of Microfluidics*, 2nd ed., Boston, MA: Integrated Microsystems Series, Artech House, 2006.
- [5] N. Kockman, *Transport Phenomena in Micro Process Engineering*. Berlin Heidelberg, Germany: Springer-Verlag, 2008.
- [6] R. M. Cotta, P. C. Pontes, A. H. R. Sousa, C. P. Naveira-Cotta and K. M. Lisboa, "Computational-analytical simulation of microsystems in process intensification," *High Temp. High Pressures, Thermophys. Prop.: Fundam. Appl.*, vol. 50, no. 6, pp. 469–495, 2021. DOI: [10.32908/hthp.v50.1189](https://doi.org/10.32908/hthp.v50.1189).
- [7] S. G. Kandlikar, S. Garimella, D. Li, S. Colin and M. R. King, *Heat Transfer and Fluid Flow in Minichannels and Microchannels*. London, UK: Elsevier, 2005.
- [8] Z. M. Zhang, *Nano/Microscale Heat Transfer. Nanoscience and Technology Series*, New York, NY: McGraw-Hill, 2007.
- [9] C. B. Sobhan and G. P. Peterson, *Microscale and Nanoscale Heat Transfer: Fundamentals and Engineering Applications*. Boca Raton, FL: CRC Press, 2008.
- [10] R. M. Cotta, D. C. Knupp and C. P. Naveira-Cotta, *Analytical Heat and Fluid Flow in Microchannels and Microsystems, Mechanical Engineering Series*. New York, NY: Springer International, 2016, DOI: [10.1007/978-3-319-23312-3](https://doi.org/10.1007/978-3-319-23312-3).
- [11] D. B. Tuckerman and R. F. W. Pease, "High performance heat sinking for VLSI," *IEEE Electron. Dev. Lett.*, vol. 2, no. 5, pp. 126–129, 1981. DOI: [10.1109/EDL.1981.25367](https://doi.org/10.1109/EDL.1981.25367).
- [12] N. H. Naquiuddin, et al., "Overview of micro-channel design for high heat flux application," *Renewable Sustainable Energy Rev.*, vol. 82, no. 1, pp. 901–914, 2018. DOI: [10.1016/j.rser.2017.09.110](https://doi.org/10.1016/j.rser.2017.09.110).
- [13] K. R. Vaddina, A. M. Rahmani, K. Latif, P. Liljeberg and J. Plosila, "Thermal modeling and analysis of advanced 3D stacked structures," *Procedia Eng.*, vol. 30, pp. 248–257, 2012. DOI: [10.1016/j.proeng.2012.01.858](https://doi.org/10.1016/j.proeng.2012.01.858).
- [14] A. Renfer, et al., "Microvortex-enhanced heat transfer in 3D-integrated liquid cooling of electronic chip stacks," *Int. J. Heat Mass Transfer*, vol. 65, pp. 33–43, 2013. DOI: [10.1016/j.ijheatmasstransfer.2013.05.066](https://doi.org/10.1016/j.ijheatmasstransfer.2013.05.066).
- [15] B. Ding, Z. H. Zhang, L. Gong, M. H. Xu and Z. Q. Huang, "A novel thermal management scheme for 3D-IC chips with multi-cores and high power density," *Appl. Therm. Eng.*, vol. 168, p. 114832, 2020. DOI: [10.1016/j.applthermaleng.2019.114832](https://doi.org/10.1016/j.applthermaleng.2019.114832).
- [16] Y. Fan and L. Luo, "Recent applications of advances in microchannel heat exchangers and multi-scale design optimization," *Heat Transfer Eng.*, vol. 29, no. 5, pp. 461–474, 2008. DOI: [10.1080/01457630701850968](https://doi.org/10.1080/01457630701850968).

- [17] W. Escher, B. Michel and D. Poulikakos, "A novel high performance, ultra thin heat sink for electronics," *Int. J. Heat Fluid Flow*, vol. 31, no. 4, pp. 586–598, 2010. DOI: [10.1016/j.ijheatfluidflow.2010.03.001](https://doi.org/10.1016/j.ijheatfluidflow.2010.03.001).
- [18] B. Ramos-Alvarado, P. Li, H. Liu and A. Hernandez-Guerrero, "CFD study of liquid-cooled heat sinks with microchannel flow field configurations for electronics, fuel cells, and concentrated solar cells," *Int. J. Energy Res.*, vol. 31, no. 14–15, pp. 2494–2507, 2011. DOI: [10.1016/j.applthermaleng.2011.04.015](https://doi.org/10.1016/j.applthermaleng.2011.04.015).
- [19] S. Zimmermann, et al., "A high-efficiency hybrid high-concentration photovoltaic system," *Int. J. Heat Mass Transfer*, vol. 89, pp. 514–521, 2015. DOI: [10.1016/j.ijheatmasstransfer.2015.04.068](https://doi.org/10.1016/j.ijheatmasstransfer.2015.04.068).
- [20] W. C. Tan, K. K. Chong and M. H. Tan, "Performance study of water-cooled multiple-channel heat sinks in the application of ultra-high concentrator photovoltaic system," *Solar Energy*, vol. 147, pp. 314–327, 2017. DOI: [10.1016/j.solener.2017.03.040](https://doi.org/10.1016/j.solener.2017.03.040).
- [21] I. F. Souza, D. C. Guerrieri, C. P. Naveira-Cotta and M. K. Tiwari, "On the thermal performance of a micro parallel channels heat exchanger," *ASME J. Thermal Sci. Eng. Appl.*, vol. 11, no. 2, p. 021006, 2019. DOI: [10.1115/1.4041439](https://doi.org/10.1115/1.4041439).
- [22] J. Fontaine, et al., "Liquid cooling of a microprocessor: Experimentation and simulation of a sub-millimeter channel heat exchanger," *Heat Transfer Eng.*, vol. 41, no. 15–16, pp. 1365–1381, 2020. DOI: [10.1080/01457632.2019.1628485](https://doi.org/10.1080/01457632.2019.1628485).
- [23] J. M. Costa Junior, et al., "An innovative metallic microfluidic device for intensified biodiesel production," *Ind. Eng. Chem. Res.*, vol. 59, no. 1, pp. 389–398, 2020. DOI: [10.1021/acs.iecr.9b04892](https://doi.org/10.1021/acs.iecr.9b04892).
- [24] G. L. Morini, "Single-phase convective heat transfer in microchannels: A review of experimental results," *Int. J. Therm. Sci.*, vol. 43, no. 7, pp. 631–651, 2004. DOI: [10.1016/j.ijthermalsci.2004.01.003](https://doi.org/10.1016/j.ijthermalsci.2004.01.003).
- [25] M. Asadi, G. Xie and B. Sundén, "A review of heat transfer and pressure drop characteristics of single and two-phase microchannels," *Int. J. Heat Mass Transfer*, vol. 79, pp. 34–53, 2014. DOI: [10.1016/j.ijheatmasstransfer.2014.07.090](https://doi.org/10.1016/j.ijheatmasstransfer.2014.07.090).
- [26] G. Maranzana, I. Perry and D. Maillet, "Mini and microchannels: Influence of axial conduction in the walls," *Int. J. Heat Mass Transfer*, vol. 47, no. 17–18, pp. 3993–4004, 2004. DOI: [10.1016/j.ijheatmasstransfer.2004.04.016](https://doi.org/10.1016/j.ijheatmasstransfer.2004.04.016).
- [27] G. Hetsroni, A. Mosyak, E. Pogrebnyak and L. P. Yarin, "Heat transfer in micro-channels: Comparison of experiments with theory and numerical results," *Int. J. Heat Mass Transfer*, vol. 48, no. 25–26, pp. 5580–5601, 2005. DOI: [10.1016/j.ijheatmasstransfer.2005.05.041](https://doi.org/10.1016/j.ijheatmasstransfer.2005.05.041).
- [28] P. Rosa, T. G. Karayiannis and M. W. Collins, "Single-phase heat transfer in microchannels: The importance of scaling effects," *Appl. Therm. Eng.*, vol. 29, no. 17–18, pp. 3447–3468, 2009. DOI: [10.1016/j.applthermaleng.2009.05.015](https://doi.org/10.1016/j.applthermaleng.2009.05.015).
- [29] J. S. Nunes, R. M. Cotta, M. R. Avelino and S. Kakaç, "Conjugated heat transfer in microchannels," *Microfluidics Based Microsystems*. Dordrecht, The Netherlands: Springer, 2010, pp. 61–82. DOI: [10.1007/978-90-481-9029-4_4](https://doi.org/10.1007/978-90-481-9029-4_4).
- [30] M. M. Mansoor, K. C. Wong and M. Siddique, "Numerical investigation of fluid flow and heat transfer under high heat flux using rectangular micro-channels," *Int. Commun. Heat Mass Transfer*, vol. 39, no. 2, pp. 291–297, 2012. DOI: [10.1016/j.icheatmasstransfer.2011.12.002](https://doi.org/10.1016/j.icheatmasstransfer.2011.12.002).
- [31] M. A. Oyinlola, G. S. F. Shire and R. W. Moss, "The significance of scaling effects in a solar absorber plate with micro-channels," *Appl. Therm. Eng.*, vol. 90, pp. 499–508, 2015. DOI: [10.1016/j.applthermaleng.2015.07.023](https://doi.org/10.1016/j.applthermaleng.2015.07.023).
- [32] A. M. Sahar, et al., "Single phase flow pressure drop and heat transfer in rectangular metallic micro-channels," *Appl. Therm. Eng.*, vol. 93, pp. 1324–1336, 2016. DOI: [10.1016/j.applthermaleng.2015.08.087](https://doi.org/10.1016/j.applthermaleng.2015.08.087).
- [33] H. Wang, Z. Chen and J. Gao, "Influence of geometric parameters on flow and heat transfer performance of micro-channel heat sinks," *Appl. Therm. Eng.*, vol. 107, pp. 870–879, 2016. DOI: [10.1016/j.applthermaleng.2016.07.039](https://doi.org/10.1016/j.applthermaleng.2016.07.039).
- [34] R. M. Cotta, "Hybrid numerical/analytical approach to nonlinear diffusion problems," *Numer. Heat Transfer, Part B: Fundam.*, vol. 17, no. 2, pp. 217–226, 1990. DOI: [10.1080/10407799008961740](https://doi.org/10.1080/10407799008961740).
- [35] R. Serfaty and R. M. Cotta, "Integral transform solutions of diffusion problems with nonlinear equation coefficients," *Int. Commun. Heat Mass Transfer*, vol. 17, no. 6, pp. 851–864, 1990. DOI: [10.1016/0735-1933\(90\)90030-N](https://doi.org/10.1016/0735-1933(90)90030-N).
- [36] R. Serfaty and R. M. Cotta, "Hybrid analysis of transient nonlinear convection-diffusion problems," *Int. J. Numer. Methods Heat Fluid Flow*, vol. 2, pp. 55–62, 1992. DOI: [10.1108/eb017479](https://doi.org/10.1108/eb017479).
- [37] R. M. Cotta, *Integral Transforms in Computational Heat and Fluid Flow*. Boca Raton, FL: CRC Press, 1993. DOI: [10.1201/9781003069065](https://doi.org/10.1201/9781003069065).
- [38] R. M. Cotta, "Benchmark results in computational heat and fluid flow: The integral transform method," *Int. J. Heat Mass Transfer*, vol. 37, no. S1, pp. 381–394, 1994. DOI: [10.1016/0017-9310\(94\)90038-8](https://doi.org/10.1016/0017-9310(94)90038-8).
- [39] R. M. Cotta and M. D. Mikhailov, *Heat Conduction - Lumped Analysis, Integral Transforms, Symbolic Computation*. Chichester, UK: Wiley, 1997.
- [40] R. M. Cotta and M. D. Mikhailov, "Hybrid methods and symbolic computations," in *Handbook of Numerical Heat Transfer*, 2nd ed., W. J. Minkowycz, E. M. Sparrow, and J. Y. Murthy, Eds. New York, NY: Wiley, 2006. DOI: [10.1002/9780470172599.ch16](https://doi.org/10.1002/9780470172599.ch16).
- [41] R. M. Cotta, D. C. Knupp, C. P. Naveira-Cotta, L. A. Sphaier and J. N. N. Quaresma, "Unified integral transforms algorithm for solving multidimensional nonlinear convection-diffusion problems," *Numer. Heat Transfer, Part A - Appl.*, vol. 63, pp. 1–27, 2013. DOI: [10.1080/10407782.2013.756763](https://doi.org/10.1080/10407782.2013.756763).
- [42] R. M. Cotta, et al., "Recent advances in computational-analytical integral transforms for convection-diffusion problems," *Heat Mass Transfer*, vol. 54, pp. 2475–2496, 2018. DOI: [10.1007/s00231-017-2186-1](https://doi.org/10.1007/s00231-017-2186-1).
- [43] R. M. Cotta, D. C. Knupp, J. N. N. Quaresma, et al., "Analytical methods in heat transfer," *Handbook of Thermal Science and Engineering*, vol. 1, F. A. Kulacki, Ed., New York, NY: Springer International

- Publishing, 2018. pp. 61–126. DOI: [10.1007/978-3-319-26695-4_2](https://doi.org/10.1007/978-3-319-26695-4_2).
- [44] M. D. Mikhailov and M. N. Ozisik, *Unified Analysis and Solutions of Heat and Mass Diffusion*. New York, NY: John Wiley and Sons Inc., 1984.
- [45] R. M. Cotta, M. D. Mikhailov and M. N. Özişik, “Transient conjugated forced convection in ducts with periodically varying inlet temperature,” *Int. J. Heat Mass Transfer*, vol. 30, no. 10, pp. 2073–2082, 1987. DOI: [10.1016/0017-9310\(87\)90087-1](https://doi.org/10.1016/0017-9310(87)90087-1).
- [46] S. Kakac, W. Li and R. M. Cotta, “Unsteady laminar forced convection in ducts with periodic variation of inlet temperature,” *ASME J. Heat Transfer*, vol. 112, no. 4, pp. 913–920, 1990. DOI: [10.1115/1.2910499](https://doi.org/10.1115/1.2910499).
- [47] R. O. C. Guedes and R. M. Cotta, “Periodic laminar forced convection within ducts including wall heat conduction effects,” *Int. J. Eng. Sci.*, vol. 29, no. 5, pp. 535–547, 1991. DOI: [10.1016/0020-7225\(91\)90059-C](https://doi.org/10.1016/0020-7225(91)90059-C).
- [48] R. O. C. Guedes, R. M. Cotta and N. C. L. Brum, “Heat transfer in laminar flow with wall axial conduction and external convection,” *J. Thermophys. Heat Transfer*, vol. 5, no. 4, pp. 508–513, 1991. DOI: [10.2514/3.294](https://doi.org/10.2514/3.294).
- [49] R. O. C. Guedes, M. N. Ozisik and R. M. Cotta, “Conjugated periodic turbulent forced convection in a parallel plate channel,” *ASME J. Heat Transfer*, vol. 116, no. 1, pp. 40–46, 1994. DOI: [10.1115/1.2910881](https://doi.org/10.1115/1.2910881).
- [50] E. J. Correa and R. M. Cotta, “Enhanced lumped-differential formulations of diffusion problems,” *Appl. Math. Model.*, vol. 22, no. 3, pp. 137–152, 1998. DOI: [10.1016/S0307-904X\(98\)00005-5](https://doi.org/10.1016/S0307-904X(98)00005-5).
- [51] J. S. Nunes, R. M. Cotta, M. R. Avelino and S. Kakaç, “Conjugated heat transfer in microchannels,” in *Microfluidics Based Microsystems: Fundamentals and Applications*, NATO Science for Peace and Security Series A: Chemistry and Biology. S. Kakaç, B. Kosoy, and A. Pramuanjaroenkij, Eds., Dordrecht, The Netherlands: Springer, 2010, pp. 61–82. DOI: [10.1007/978-90-481-9029-4_4](https://doi.org/10.1007/978-90-481-9029-4_4).
- [52] D. C. Knupp, C. P. Naveira-Cotta and R. M. Cotta, “Theoretical analysis of conjugated heat transfer with a single domain formulation and integral transforms,” *Int. Commun. Heat Mass Transfer*, vol. 39, no. 3, pp. 355–362, 2012. DOI: [10.1016/j.icheatmasstransfer.2011.12.012](https://doi.org/10.1016/j.icheatmasstransfer.2011.12.012).
- [53] D. C. Knupp, R. M. Cotta and C. P. Naveira-Cotta, “Heat transfer in microchannels with upstream-downstream regions coupling and wall conjugation effects,” *Numer. Heat Transfer, Part B: Fundam.*, vol. 64, no. 5, pp. 365–387, 2013. DOI: [10.1080/10407790.2013.810535](https://doi.org/10.1080/10407790.2013.810535).
- [54] D. C. Knupp, C. P. Naveira-Cotta and R. M. Cotta, “Conjugated convection-conduction analysis in micro-channels with axial diffusion effects and a single domain formulation,” *ASME J. Heat Transfer*, vol. 135, no. 9, p. 091401, 2013. DOI: [10.1115/1.4024425](https://doi.org/10.1115/1.4024425).
- [55] D. C. Knupp, C. P. Naveira-Cotta and R. M. Cotta, “Unified integral transforms in single domain formulation for internal flow three-dimensional conjugated problems,” International Heat Transfer Conference Digital Library, IHTC 2014, 2014. Begel House Inc., pp. 1–14. DOI: [10.1615/IHTC15.nsm.009729](https://doi.org/10.1615/IHTC15.nsm.009729).
- [56] D. C. Knupp, R. M. Cotta, C. P. Naveira-Cotta and S. Kakaç, “Transient conjugated heat transfer in micro-channels: Integral transforms with single domain formulation,” *Int. J. Therm. Sci.*, vol. 88, pp. 248–257, 2015. DOI: [10.1016/j.ijthermalsci.2014.04.017](https://doi.org/10.1016/j.ijthermalsci.2014.04.017).
- [57] D. C. Knupp, R. M. Cotta and C. P. Naveira-Cotta, “Fluid flow and conjugated heat transfer in arbitrarily shaped channels via single domain formulation and integral transforms,” *Int. J. Heat Mass Transfer*, vol. 82, pp. 479–489, 2015. DOI: [10.1016/j.ijheatmasstransfer.2014.11.007](https://doi.org/10.1016/j.ijheatmasstransfer.2014.11.007).
- [58] J. L. Z. Zotin, D. C. Knupp and R. M. Cotta, “Conjugated heat transfer in complex geometries via total integral transformation and single domain formulation,” 4th Int. Conf. Comput. Methods Therm. Prob., ThermaComp2016, July 2016, pp. 1–4, Atlanta, USA.
- [59] J. L. Z. Zotin, D. C. Knupp and R. M. Cotta, “Conjugated heat transfer in complex channel-substrate configurations: Hybrid solution with total integral transformation and single domain formulation,” Proc. ITherm 2017 - Sixteenth Intersoc. Conf. Therm. Thermomech. Phenomena Electron. Syst., Paper #435, pp. 184–191. Orlando, FL, USA, May 30th –June 2nd, 2017. DOI: [10.1109/ITHEM.2017.7992470](https://doi.org/10.1109/ITHEM.2017.7992470).
- [60] D. C. Knupp, F. S. Mascouto, L. A. S. Abreu, C. P. Naveira-Cotta and R. M. Cotta, “Conjugated heat transfer in circular microchannels with slip flow and axial diffusion effects,” *Int. Commun. Heat Mass Transfer*, vol. 91, pp. 225–233, 2018. DOI: [10.1016/j.icheatmasstransfer.2017.12.003](https://doi.org/10.1016/j.icheatmasstransfer.2017.12.003).
- [61] D. C. Knupp, R. M. Cotta and C. P. Naveira-Cotta, “Conjugate heat transfer: Analysis via integral transforms and eigenvalue problems,” *J. Eng. Phys. Thermophys.*, vol. 93, no. 1, pp. 60–73, 2020. DOI: [10.1007/s10891-020-02091-x](https://doi.org/10.1007/s10891-020-02091-x).
- [62] F. V. Castellões and R. M. Cotta, “Analysis of transient and periodic convection in microchannels via integral transforms,” *Prog. Comput. Fluid Dyn.*, vol. 6, no. 6, pp. 321–326, 2006. DOI: [10.1504/PCFD.2006.010772](https://doi.org/10.1504/PCFD.2006.010772).
- [63] T. Persoons, T. Saenen, T. van Oevelen and M. Baelmans, “Effect of flow pulsation on the heat transfer performance of a minichannel heat sink,” *ASME J. Heat Transfer*, vol. 134, no. 9, pp. 1–7, 2012. DOI: [10.1115/1.4006485](https://doi.org/10.1115/1.4006485).
- [64] A. H. Altun, Ş. Bilir and A. Ateş, “Transient conjugated heat transfer in thermally developing laminar flow in thick walled pipes and minipipes with time periodically varying wall temperature boundary condition,” *Int. J. Heat Mass Transfer*, vol. 92, pp. 643–657, 2016. DOI: [10.1016/j.ijheatmasstransfer.2015.09.011](https://doi.org/10.1016/j.ijheatmasstransfer.2015.09.011).
- [65] S. Şen and S. Darici, “Transient conjugate heat transfer in a circular microchannel involving rarefaction, viscous dissipation and axial conduction effects,” *Appl. Therm. Eng.*, vol. 111, pp. 855–862, 2017. DOI: [10.1016/j.applthermaleng.2016.10.005](https://doi.org/10.1016/j.applthermaleng.2016.10.005).
- [66] K. Ghule and M. S. Soni, “Numerical heat transfer analysis of wavy micro channels with different cross sections,” *Energy Procedia*, vol. 109, pp. 471–478, 2017. DOI: [10.1016/j.egypro.2017.03.071](https://doi.org/10.1016/j.egypro.2017.03.071).

- [67] R. M. Cotta, C. P. Naveira-Cotta and D. C. Knupp, “Enhanced eigenfunction expansions in convection-diffusion problems with multiscale space variable coefficients,” *Numer. Heat Transfer, Part A - Appl.*, vol. 70, no. 5, pp. 492–512, 2016. DOI: [10.1080/10407782.2016.1177342](https://doi.org/10.1080/10407782.2016.1177342)
- [68] R. M. Cotta, D. C. Knupp, C. P. Naveira-Cotta, L. A. Sphaier and J. N. N. Quaresma, “The unified integral transforms (UNIT) algorithm with total and partial transformation,” *Comput. Therm. Sci.*, vol. 6, no. 6, pp. 507–524, 2014. DOI: [10.1615/ComputThermalScien.2014008663](https://doi.org/10.1615/ComputThermalScien.2014008663).
- [69] C. P. Naveira-Cotta, R. M. Cotta and H. R. B. Orlande, “Inverse analysis with integral transformed temperature fields for identification of thermophysical properties functions in heterogeneous media,” *Int. J. Heat Mass Transfer*, vol. 54, no. 7–8, pp. 1506–1519, 2011. DOI: [10.1016/j.ijheatmasstransfer.2010.11.042](https://doi.org/10.1016/j.ijheatmasstransfer.2010.11.042).
- [70] L. A. S. Abreu, et al., “Detection of contact failures with the Markov Chain Monte Carlo method by using integral transformed measurements,” *Int. J. Therm. Sci.*, vol. 132, pp. 486–497, 2018. DOI: [10.1016/j.ijthermalsci.2018.06.006](https://doi.org/10.1016/j.ijthermalsci.2018.06.006).